INFECTION AND IMMUNITY, Mar. 2010, p. 1193–1201 Vol. 78, No. 3
0019-9567/10/$12.00 doi:10.1128/IAI.00932-09

Shiga Toxin 1-Induced Inflammatory Response in Lipopolysaccharide-Sensitized Astrocytes Is Mediated by Endogenous Tumor Necrosis Factor Alpha[▽]

Verónica I. Landoni,[1,3]* Marcelo de Campos-Nebel,[2] Pablo Schierloh,[1] Cecilia Calatayud,[4] Gabriela C. Fernandez,[1,3] M. Victoria Ramos,[1,3] Bárbara Rearte,[1,3] Marina S. Palermo,[1,3] and Martín A. Isturiz[1,3]

Departamento de Inmunología,[1] and Departamento de Genética,[2] Academia Nacional de Medicina, and Instituto de Leucemia Experimental, CONICET,[3] and Química Biológica, Facultad de Farmacia y Bioquímica, Universidad de Buenos Aires,[4] Ciudad Autónoma de Buenos Aires, Argentina

Received 15 August 2009/Returned for modification 23 September 2009/Accepted 3 December 2009

Hemolytic-uremic syndrome (HUS) is generally caused by Shiga toxin (Stx)-producing *Escherichia coli*. Endothelial dysfunction mediated by Stx is a central aspect in HUS development. However, inflammatory mediators such as bacterial lipopolysaccharide (LPS) and polymorphonuclear neutrophils (PMN) contribute to HUS pathophysiology by potentiating Stx effects. Acute renal failure is the main feature of HUS, but in severe cases, patients can develop neurological complications, which are usually associated with death. Although the mechanisms of neurological damage remain uncertain, alterations of the blood-brain barrier associated with brain endothelial injury is clear. Astrocytes (ASTs) are the most abundant inflammatory cells of the brain that modulate the normal function of brain endothelium and neurons. The aim of this study was to evaluate the effects of Stx type 1 (Stx1) alone or in combination with LPS in ASTs. Although Stx1 induced a weak inflammatory response, pretreatment with LPS sensitized ASTs to Stx1-mediated effects. Moreover, LPS increased the level of expression of the Stx receptor and its internalization. An early inflammatory response, characterized by the release of tumor necrosis factor alpha (TNF-α) and nitric oxide and PMN-chemoattractant activity, was induced by Stx1 in LPS-sensitized ASTs, whereas activation, evidenced by higher levels of glial fibrillary acid protein and cell death, was induced later. Furthermore, increased adhesion and PMN-mediated cytotoxicity were observed after Stx1 treatment in LPS-sensitized ASTs. These effects were dependent on NF-κB activation or AST-derived TNF-α. Our results suggest that TNF-α is a pivotal effector molecule that amplifies Stx1 effects on LPS-sensitized ASTs, contributing to brain inflammation and leading to endothelial and neuronal injury.

The epidemic form of hemolytic-uremic syndrome (HUS) has been associated with enterohemorrhagic infections caused by Shiga toxin (Stx)-producing *Escherichia coli* (STEC) organisms (33). HUS is the most common cause of acute renal failure in children and is related to the endothelial damage of glomeruli and/or arterioles of the kidney and epithelial cell damage induced by Stx through the interaction with its globotriaosylceramide (Gb_3) receptor (35). Although Stx is the main pathogenic factor and is necessary for epidemic HUS development, clinical and experimental evidence suggests that the inflammatory response is able to potentiate Stx toxicity. In fact, both bacterial lipopolysaccharide (LPS) and polymorphonuclear neutrophils (PMN) play a key role in the full development of HUS (15). Moreover, PMN leukocytosis in patients correlates with a poor prognosis (17).

Endothelial cell damage is not limited to the kidney but extends to other organs; in severe cases, the brain can be affected. In fact, central nervous system (CNS) complications indicate severe HUS, and brain damage involvement is the most common cause of death (14).

However, the pathogenesis of CNS impairment is not yet fully understood. Although it has been demonstrated that human brain endothelial cells (BECs) are relatively resistant to Stx, inflammatory mediators, such as tumor necrosis factor alpha (TNF-α), markedly increase human BEC sensitivity to Stx cytotoxicity (11).

BECs are part of the blood-brain barrier (BBB), which protects the brain from potentially harmful substances and leukocytes present in the bloodstream. Thus, the integrity of BBB function is theorized to be a key component in CNS-associated pathologies, and BEC damage is thought to be one of the possible mechanisms involved in the disruption of the BBB in HUS. In fact, LPS from bacterial infections leads to the release of TNF-α, interleukin-1β (IL-1β), and reactive oxygen species (ROS), all of which have the ability to open the BBB.

Several *in vivo* studies demonstrated previously that Stx is able to impair BBB function, increasing its permeability (21). Moreover, Stx itself is able to cross the endothelial barrier and enter into the CNS, since Stx activity in cerebrospinal fluid was previously observed (19, 23), and Stx was previously immunodetected in many brain cells including astrocytes (ASTs) and neurons (44).

* Corresponding author. Mailing address: Departamento de Inmunología, Academia Nacional de Medicina, Pacheco de Melo 3081, 1425 Buenos Aires, Argentina. Phone: 5411-48055579. Fax: 5411-48039475. E-mail: vilandoni@yahoo.com.ar.
▽ Published ahead of print on 14 December 2009.

ASTs, which are inflammatory cells found throughout the CNS, are in close contact with BECs by end-foot processes (24), and their interaction with the cerebral endothelium determines BBB function (2, 4). In addition, ASTs interact with neurons through gap junctions and release neurotrophins that are essential for neuronal survival (6). However, in response to brain injury, ASTs become activated and release inflammatory mediators such as nitric oxide (NO) and TNF-α, altering the permeability of the BBB and affecting neuronal survival and tissue integrity (1, 9). In addition, AST-derived cytokines and chemokines can stimulate the peripheral immune system and attract peripheral inflammatory leukocytes to the site of injury (46).

ASTs are therefore in a critical position to influence neuronal viability and BEC integrity once Stx and factors associated with the STEC infection reach the brain parenchyma. We hypothesize that the effects of LPS and Stx on ASTs may be involved in the brain damage observed with severe cases of HUS. Thus, the aim of this study was to evaluate whether Stx type 1 (Stx1) alone or in combination with LPS is capable of inducing an inflammatory response in ASTs.

MATERIALS AND METHODS

AST isolation and PMN purification. ASTs were prepared from rat cerebral tissue cortex as previously described (27). Briefly, cerebral hemispheres were dissected out from newborn rats, freed of meninges, and dissociated by gentle pipetting on Dulbecco's modified Eagle's medium (DMEM)-Ham's F12 medium (1:1, vol/vol) (Gibco, Invitrogen, Argentina) containing 5 μg/ml streptomycin and 5 U/ml penicillin supplemented with 10% fetal calf serum (FCS) (Gibco). The cell suspensions were seeded into poly-L-lysine-coated 75-cm^2 tissue culture flasks (Corning, New York, NY). After 14 days of culture, ASTs were separated from microglia and oligodendrocytes by shaking twice, for 24 h each, in an orbital shaker. The purity of AST cultures was 90 to 95% (glial fibrillary acidic protein [GFAP]-positive staining by flow cytometry analysis).

PMN were isolated from heparinized blood from adult rats. PMN were collected following Ficoll-Hypaque gradient centrifugation and 6% dextran sedimentation. Viability was assessed by trypan blue exclusion, and purity was determined by Turk's solution staining. Only fractions containing at least 80% PMN were used.

Stx1 preparation. Stx1 was kindly provided Sugiyama Junichi (Denka Seiken Co. Ltd., Nigata, Japan). Purity was analyzed by the supplier, showing only one peak by high-performance liquid chromatography (HPLC). The Stx1 preparation was checked for endotoxin contamination by the *Limulus* amoebocyte lysate assay containing less than 40 pg lipopolysaccharide (LPS)/μg of Shiga toxin protein.

Cell culture and treatments. ASTs (7×10^4) were seeded into 24-well plates and cultured in DMEM containing 10% FCS and supplemented with 5 μg/ml streptomycin and 5 U/ml penicillin. Cultures were maintained at 37°C in a humidified 5% CO_2 atmosphere. After 24 h, ASTs were mock treated (control) or treated with LPS (0.5 μg/ml), Stx1 (10 ng/ml), or LPS plus Stx1 (Stx1 added 18 h after LPS). Purified LPS derived from *E. coli* O111:B4 (Sigma) was used.

The NF-κB inhibitor (*E*)-3-(4-methylphenylsulfonyl)-2-propenenitril (BAY11-7082; Biomol, Plymouth Meeting, PA) was used for suppressing NF-κB activation. A total of 40 μM BAY11-7082 was added to AST cultures 30 min before treatment.

A soluble tumor necrosis factor receptor (etanercept) (Enbrel; Wyeth Inc., Collegeville, PA) was used to block the action of AST-secreted TNF-α. A total of 5 ng/ml was added to AST cultures 10 min before treatment.

Cell-free conditioned medium from untreated (control)-, LPS-, Stx1-, or LPS- and Stx1-treated ASTs was collected 24 h after treatment with Stx1 and analyzed for TNF-α and NO production or used as chemotaxis stimulus for PMN migration assays.

Cell death analysis. The cell death analysis of untreated (control) or LPS-, Stx1-, or LPS- and Stx1-treated ASTs was performed at 24, 48, and 72 h after treatment with Stx1. Detached dead cells were carefully collected along with undetached cells. An annexin V (AV)-fluorescein isothiocyanate (FITC) apoptosis detection kit (Calbiochem) was used according to the manufacturer's instructions. Briefly, ASTs were incubated for 30 min with medium binding reagent and FITC-labeled AV (1 μg/ml) in the dark at room temperature. Cells were washed, resuspended in medium binding buffer, and incubated for 10 min with propidium iodide (PI) (15 μg/ml). The percentage of PI-positive (PI^+) $AV^{+/-}$ (PI^+/AV^- plus PI^+/AV^+) and PI^- AV^+ cells was determined by flow cytometry using a FACScan cytometer (Becton Dickinson). Analysis was performed by using CellQuest (Becton Dickinson) or FCS Express (De Novo Software, Los Angeles, CA) software. At least 30,000 events were evaluated per sample.

GFAP expression. The levels of GFAP of untreated (control) or LPS-, Stx1-, or LPS- and Stx1-treated ASTs were determined by fluorescence-activated cell sorter (FACS) analysis at 24, 48, and 72 h of treatment with Stx1. Cultures were first washed in order to remove detached dead cells and debris. Harvested ASTs were fixed with 2% paraformaldehyde and permeabilized with 0.25% Triton X-100 at room temperature for 20 min. After blocking (3% bovine serum albumin [BSA] and 0.25% Triton X-100 in phosphate-buffered saline [PBS]) for 1 h, samples were incubated for 2 h with IgY chicken anti-GFAP (1:300 dilution; Neuromics, Edina, MN). After washing, appropriate secondary FITC-conjugated goat anti-chicken IgY antibody (1:250 dilution; Neuromics, Edina, MN) was added and incubated for 1 h. Immunostaining was analyzed by FACS analysis. The analysis gate was set on GFAP-positive cells.

Gb_3 analysis. The cell surface expression of the Stx1 receptor Gb_3 (CD77) was evaluated by flow cytometry analysis of mock-treated or treated ASTs (LPS, Stx1, or LPS and Stx1 treatment). The analysis was performed at 24 h of treatment with Stx1. ASTs were harvested, blocked with 3% BSA for 20 min, and exposed to anti-human CD77 monoclonal antibody (1:100 dilution; Immunotech) for 45 min at 4°C. Unstimulated cells, incubated with anti-human isotype mouse IgM, were used as a negative control. Cells were washed and incubated with a secondary antibody, FITC $F(ab')_2$ goat anti-mouse IgM, mu chain (1:250 dilution; BD Pharmingen), in the dark for 30 min at 4°C. Washed cells were immediately analyzed by FACS.

Stx1 binding and internalization analysis. ASTs were rapidly harvested, fixed, and permeabilized with 2% paraformaldehyde containing 0.25% Triton X-100 for 20 min at room temperature. After blocking (3% BSA and 0.25% Triton X-100 in PBS) for 1 h at 4°C, samples were incubated for 2 h with mouse IgG1 anti-Stx1 (1:200 dilution; Toxin Technology, Sarasota, FL) or the corresponding isotype. ASTs were then incubated with a secondary FITC anti-mouse antibody (1:100 dilution; Bio-Rad Laboratories, Hercules, CA) for 40 min at 4°C. The internalization index was determined by FACS by normalizing the mean fluorescence intensity (MFI) value of treated-AST binding/internalization at 37°C to the MFI binding value at 4°C.

L929 cytotoxicity bioassay. A modified L929 cytotoxic bioassay system for TNF-α quantification was employed to evaluate secreted TNF-α in treated ASTs (37). Briefly, 2×10^4 L929 cells per well were seeded into a 96-well tissue culture plate and cultured in RPMI medium supplemented with 5 μg/ml streptomycin, 5 U/ml penicillin, and 10% FCS. The medium was replaced with 0.1 ml of medium alone, AST-derived supernatants, or rat recombinant TNF-α standard. The L929 cells were grown in the presence of actinomycin D (10 μg/ml; Amersham Biosciences). After 24 h of incubation, the cells were washed with PBS, and viable cells were fixed and stained with 0.2% crystal violet in 20% methanol for 20 min at 37°C. Samples were washed and lysed with 30% acetic acid solution. The resultant absorbance (Abs) was measured with a microtiter plate reader (Organon Tecnika, Argentina) at 550 nm. Bioactive TNF-α was expressed as a percentage of L929 cytotoxicity. This percentage of L929 cytotoxicity was calculated by the following formula: percent L929 cytotoxicity = 100 × (Abs of 100% viable cells in control wells − Abs of test wells)/(Abs of 100% viable cells in control wells).

Nitrite quantification. NO production was determined by the measurement of nitrite in cell free-supernatants from treated ASTs using the Griess reaction. Briefly, 50 μl of sample aliquots was mixed with 50 μl of Griess reagent (1% sulfanilamide–0.1% naphthylethylene diamine dihydrochloride–2% phosphoric acid) in 96-well plates and incubated at 25°C for 10 min. The absorbance at 540 nm was measured with a microplate reader. $NaNO_2$ was used as a standard to calculate nitrite concentrations.

PMN chemotaxis assay. Neutrophil chemotaxis was quantified by using a modification of the Boyden chamber technique (5). A cell suspension (50 μl) containing 2×10^6 cells/ml in RPMI medium (Gibco) with 0.5% BSA was placed into the top wells of a 48-well microchemotaxis chamber. A polyvinylpyrrolidone (PVP)-free polycarbonate membrane (3-μm pore size; Neuro Probe Inc.) separated the cells from lower wells containing either DMEM or treated-AST conditioned medium. The chamber was incubated for 90 min at 37°C in a 5% CO_2 humidified atmosphere. After incubation, the filter was stained with Tincion-15 (Biopur SRL, Argentina), and the number of PMN on the undersurface of the

filter was counted in five random high-power fields (HPF) at a magnification of ×400 for each of triplicate filters.

PMN adhesion and cytotoxicity. Purified PMN were seeded over treated ASTs in a PMN/AST ratio of 1:20 and cultured for 3 h for adhesion or 8 h for cytotoxicity analysis. Nonadherent PMN were removed by vigorous washing from the plates with PBS four times, and adherent cells were stained with May Grunwald-Giemsa stain. Three random fields per treatment were photographed in each experiment (Nikon Coolpix 4500 digital camera) under a ×600 magnification (Nikon Eclipse TE2000-S inverted microscope). The number of adherent PMN (for the adhesion assay) or the number of remnant ASTs (for the PMN-mediated cytotoxicity assay) on each photograph was counted by using ImageJ software (National Institutes of Health, Bethesda, MD). The number of ASTs bearing PMN was scored in three randomly selected microscope fields (~50 ASTs; $n = 3$). Data were grouped as the number of ASTs with <3, 3 to 6, or >7 adhered PMN. Stratified distribution analyses of these data were use for statistical analysis. The percent PMN-mediated AST cytotoxicity was calculated as follows: percent cytotoxicity = 100 − [(number of treated ASTs/number of untreated ASTs) × 100].

Statistical analysis. Statistical differences among treatments were determined by using a paired *t* test for two-group comparisons and a paired one-way analysis of variance (ANOVA) followed by the Bonferroni posttest for multiple comparisons. A chi-squared (χ^2) test for trends was applied to the PMN adhesion assay. A P value of <0.05 was considered to be significant. All tests were carried out by using Prism 5.0 software (Graph Pad Software, La Jolla, CA).

RESULTS

LPS pretreatment sensitizes ASTs to Stx1-mediated effects. The biological activity of Stx involves the inhibition of protein synthesis, leading to cell death (12). Therefore, we first determined if Stx1 was able to induce toxicity on ASTs and evaluated the LPS modulation of Stx1-induced effects by priming ASTs with LPS for 18 h before adding Stx1. Cell death was determined by FACS analysis using annexin V (AV) and propidium iodide (PI) in cultures at different times. As shown in Fig. 1A, Stx1 (10 ng/ml) alone did not induce significant cell death, even when higher doses of Stx1 (25 ng/ml and 100 ng/ml) were used (data not shown). However, when ASTs were preincubated with LPS, Stx1 (10 ng/ml) induced a slight but statistically significant increase in the percentage of cell death ($PI^+/AV^{+/-}$ plus PI^-/AV^+) at 48 and 72 h. Higher-level and similar toxic effects were observed with both 25 and 100 ng/ml of Stx1 (~30% of cell death) in LPS-treated ASTs (data not shown).

The hallmark of AST activation is the enhanced expression of the major intermediate filament protein, glial fibrillary acidic protein (GFAP) (13). As depicted in Fig. 1B, Stx1 induced the upregulation of GFAP in LPS-sensitized ASTs at 72 h. However, Stx1 alone was not sufficient to increase the level of GFAP expression. The same results were obtained when higher doses of Stx1 were used (25 ng/ml and 100 ng/ml) alone or in combination with LPS (data not shown). These data were validated by parallel observations by epifluorescence microscopy (data not shown). Together, our results show that Stx1 induces cytotoxicity and activation only in LPS-sensitized ASTs.

Given the above-described results, for subsequent experiments, we choose the minimal dose of Stx1 (10 ng/ml) that, in combination with LPS, induced maximal cell activation with minor toxic effects.

Expression of Stx1 receptor and Stx1 internalization are increased in LPS-sensitized ASTs. Proinflammatory stimuli are known to increase the expression of the Stx1 receptor Gb_3 on the surface of different Stx1 target cells *in vitro* (36). The

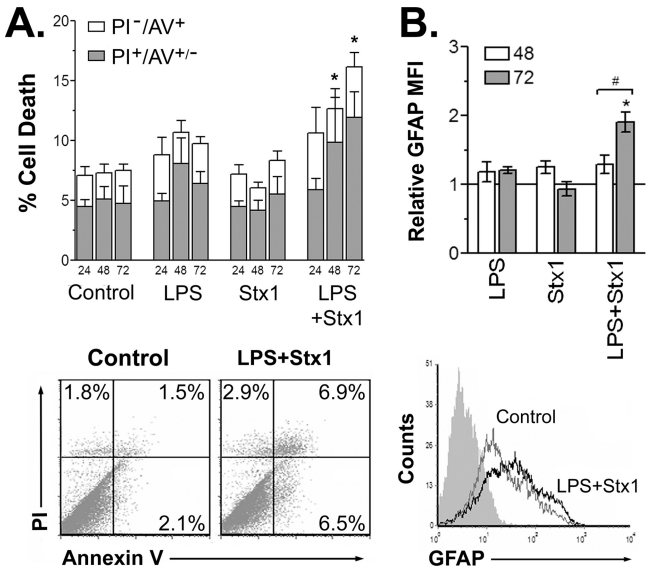

FIG. 1. Stx1-mediated effects are enhanced in LPS-sensitized ASTs. ASTs were cultured in complete medium alone (control) or in the presence of 0.5 μg/ml LPS (0 to 72 h) and/or 10 ng/ml Stx1 (18 h after LPS pretreatment). Cell death evaluation (A) and intracellular GFAP immunolabeling (B) were determined by FACS analysis. (A) Percent cell death (mean ± standard error of the mean [SEM]) measured as percent $PI^+/AV^{+/-}$ (PI^+/AV^- plus PI^+/AV^+) and PI^-/AV^+ cells after 24, 48, and 72 h of treatment with Stx1. *, $P < 0.01$ for treatment with LPS and Stx1 versus the control ($n = 4$). (Bottom) Dot plot analysis of one representative experiment at 72 h. (B) Relative (to control) median fluorescence intensity (MFI) of intracellular GFAP immunostaining (mean ± SEM) measured 48 h (white bars) and 72 h (gray bars) after Stx1 treatment. *, $P < 0.01$ for treatment with LPS and Stx1 versus the control; #, $P < 0.05$ for LPS plus Stx1 at 48 h versus LPS plus Stx1 at 72 h ($n = 5$). Histogram plot of one representative experiment at 72 h showing untreated AST (control) and LPS- and Stx1-treated AST (LPS+Stx1) MFI of GFAP. The gray-filled histogram represents the isotype control (bottom).

FACS analysis depicted in Fig. 2A shows that LPS stimulated Gb_3 expression on ASTs. In addition, although Stx1 alone failed to enhance Gb_3 expression, Stx1 induced maximal Gb_3 expression in LPS-sensitized ASTs. To determine if the enhanced Gb_3 expression correlated with increased toxin internalization, we evaluated Stx1 uptake in LPS-sensitized ASTs by FACS analysis by permeabilizing ASTs after 30 min of Stx1 (30 ng/ml) exposure at 37°C or 4°C (for background binding estimations). As shown in Fig. 2B, although ASTs were able to internalize Stx1, a significant increase in the level of toxin uptake was observed for LPS-sensitized ASTs ($P = 0.04$).

These results indicate that LPS priming of ASTs induces an increased level of Gb_3 surface expression, and this is associated with a higher Stx1 internalization rate.

The inflammatory response induced by Stx1 is enhanced in LPS-sensitized ASTs. ASTs are an important source of cytokines and chemokines that play a role in brain inflammatory responses. Thus, we assessed whether Stx1, alone or after LPS sensitization, was able to elicit an inflammatory response in ASTs. We determined the levels of secretion of TNF-α and NO production in AST conditioned medium, since both are known to be implicated in neurodegenerative and neuroinflammatory conditions (16, 31). As shown in Fig. 3A, ASTs

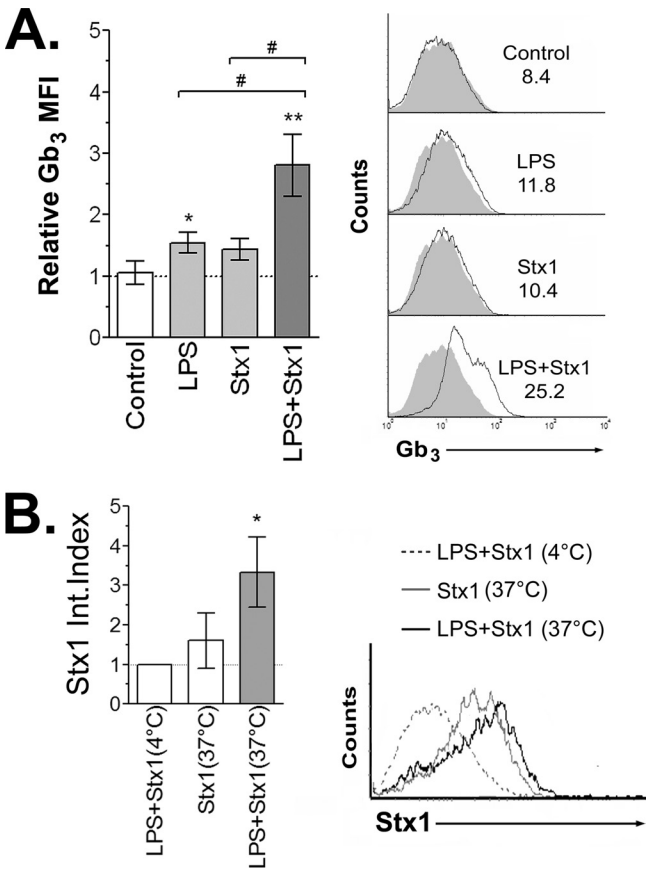

FIG. 2. LPS increases levels of Gb_3 expression and Stx1 internalization in ASTs. ASTs were cultured in complete medium alone (control) or in the presence of 0.5 μg/ml LPS (0 to 42 h) and/or 10 ng/ml Stx1 (18 h after LPS pretreatment). Evaluation of Gb_3 levels (A) and Stx1 internalization (B) was performed by FACS analysis. (A) Relative (to isotype) MFI of the Stx1 receptor Gb_3 (mean ± SEM) measured at 24 h following treatment with Stx1. **, $P < 0.005$ for LPS and Stx1 versus the control; *, $P < 0.05$ for LPS versus the control; #, $P < 0.01$ for LPS and Stx1 versus Stx1 or LPS ($n = 4$). Histogram plots from one representative experiment are presented (right). Gray-filled histograms represent the isotype control. (B) Differential Stx1 internalizations between untreated (control) and LPS-sensitized ASTs were determined by incubating cell cultures with Stx1 during 30 min at 37°C before intracellular staining and FACS analysis. A 4°C incubation was performed in parallel in order to estimate the surface binding of Stx1. The internalization index (Stx1 Int.Index) was calculated by normalizing the MFI of treated ASTs at 37°C to the MFI values at 4°C. *, $P < 0.05$ for LPS versus the control ($n = 3$). A histogram plot of one representative experiment is shown (right).

treated with either Stx1 or LPS alone secreted significant amounts of TNF-α compared to control AST conditioned medium. However, maximal TNF-α activity was detected in conditioned medium from Stx1- and LPS-sensitized ASTs. As depicted in Fig. 3B, the level of NO production by ASTs was significantly increased by LPS treatment. Furthermore, when Stx1 was added to LPS-sensitized ASTs, a higher level of production of NO was observed.

Consistent with an upregulation of proinflammatory mediator expression, peripheral blood cell infiltration is a prominent postinjury event in brain pathologies. In addition, a deleterious role of PMN in HUS was previously suggested (15). This prompted us to determine whether treated ASTs were able to release chemoattracting factors for PMN. For this purpose, conditioned media from treated ASTs were used as chemotactic stimuli, and the number of migrated PMN was determined by using a chemotaxis chamber. Figure 3C shows that conditioned medium from ASTs treated with LPS or Stx1 alone induced a statistically significant chemotaxis of PMN compared to untreated-AST conditioned medium. The highest level of PMN migration was obtained when LPS-treated ASTs were stimulated with Stx1. LPS or Stx1 alone was not a chemoattractant by itself (data not shown). Taken together, these results suggest that Stx1 induces an inflammatory response that is enhanced by LPS priming.

Levels of PMN adhesion and PMN-mediated cytotoxicity induced by Stx1 are increased in LPS-sensitized ASTs. Since PMN release several toxic mediators that have the potential to damage brain tissue (3), and given the above-described results, we evaluated the interactions and effects of PMN on treated ASTs. We first investigated the adhesiveness of PMN to stimulated ASTs (20:1 ratio of PMN/ASTs) by scoring the number of PMN physically associated with ASTs by light microscopy. As depicted in Fig. 4A, most of the untreated ASTs bound only small numbers of PMN (mean adhesion, ~2.1 PMN/AST), while a large amount of Stx1- or LPS-treated ASTs bound low or intermediate numbers of PMN (mean adhesion of ~3.5 PMN/AST for Stx1-treated ASTs and mean adhesion of ~4.2 PMN/AST for LPS-treated ASTs). Maximal Stx1-induced PMN adhesion was observed for LPS-sensitized ASTs (mean adhesion of ~7.4 PMN/AST for LPS- and Stx1-treated ASTs).

To further evaluate the potential damage induced by PMN, the percentage of cytotoxicity was evaluated for ASTs cocultured with PMN (ratio of PMN/ASTs of 20:1). Results summarized in Fig. 4B indicate that the addition of PMN after LPS or Stx1 stimulation resulted into a significant increase in AST toxicity compared to that of PMN alone. However, maximal PMN-mediated cytotoxicity was observed for LPS- and Stx1-treated ASTs.

Inhibition of NF-κB or blockade of TNF-α activity abrogates effects mediated by Stx1 in LPS-sensitized ASTs. LPS triggers a signaling cascade that results in the activation and nuclear translocation of the transcription factor NF-κB that regulates proinflammatory genes including TNF-α family members (30). In addition, following damage to the central nervous system (CNS), many processes occurring in reactive ASTs are regulated largely by NF-κB.

In order to determine whether the enhanced effects observed for Stx1- and LPS-treated ASTs were mediated by NF-κB activation, the experiments described in Fig. 1, 2, and 3A and C were performed in the presence of BAY11-7082, an inhibitor of NF-κB activation. In parallel, the contribution of endogenously secreted TNF-α was also evaluated by the addition of a soluble TNF-α receptor (etanercept) before the LPS sensitization of ASTs. Etanercept, at the concentrations used in this study, inhibited the cytotoxic activity of recombinant rat TNF-α in L929 cells (data not shown).

Figure 5A shows that the suppression of NF-κB by 40 μM BAY11-7082 or TNF-α blockade with 5 ng/ml of etanercept in ASTs treated with LPS and Stx1 resulted in a complete inhibition of TNF-α activity when conditioned medium was used to determine TNF-α secretion by the L929 bioassay. Cell death

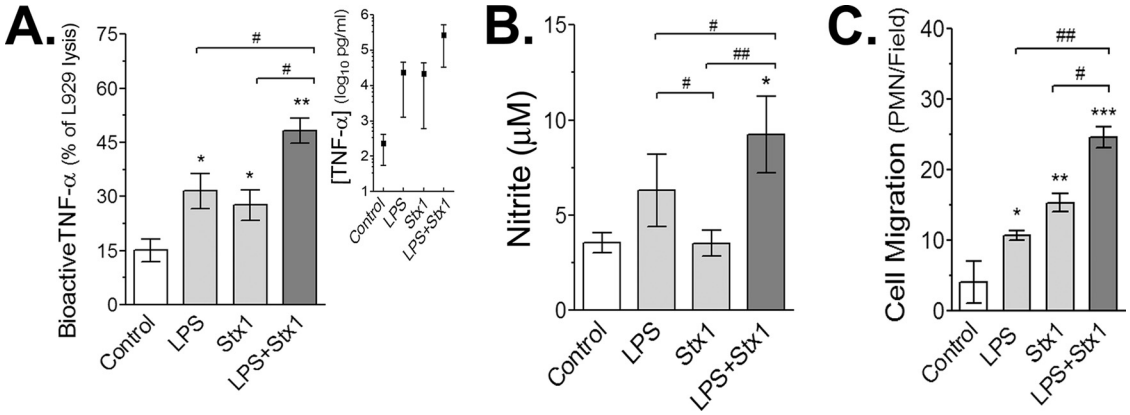

FIG. 3. Stx1 induces an inflammatory response in ASTs. ASTs were cultured in complete medium alone (control) or in the presence of 0.5 μg/ml LPS (0 to 42 h) and/or 10 ng/ml Stx1 for 24 h (added 18 h after LPS pretreatment). Culture conditioned medium was collected 24 h following Stx1 treatment for TNF-α bioassay (A), nitric oxide production (B), or PMN chemotactic migration assay (C). (A) TNF-α activity was estimated by the L929 cytotoxic assay as percent cell lysis (mean ± SEM). **, $P < 0.001$ for LPS and Stx1 versus the control; *, $P < 0.05$ for LPS or Stx1 versus the control; #, $P < 0.05$ for LPS and Stx1 versus Stx1 or LPS ($n = 9$). (Inset) The TNF-α concentration (mean ± SEM) ($n = 5$) was estimated in the same bioassays by interpolation to recombinant rat TNF-α standard curves. (B) Nitric oxide production was estimated by determining the nitrite concentration (mean ± SEM). *, $P < 0.02$ for LPS and Stx1 versus the control; ##, $P < 0.01$ for LPS and Stx1 versus Stx1; #, $P < 0.05$ for LPS and Stx1 or Stx1 versus LPS ($n = 6$). (C) Cell migration was determined by using a PMN chemotaxis assay. The number of migrated PMN was measured by light microscopy of five random high-power fields (magnification, ×400) (mean ± SEM). ***, $P < 0.005$ for LPS and Stx1 versus the control; **, $P < 0.01$ for Stx1 versus the control; *, $P < 0.01$ for LPS versus the control; #, $P < 0.02$ for LPS and Stx1 versus Stx1; ##, $P < 0.005$ for LPS and Stx1 versus LPS ($n = 4$).

mediated by Stx1 in LPS-sensitized ASTs was abolished in the presence of either BAY11-7082 or etanercept (Fig. 5B). Consistently, AST activation (Fig. 5C) and the secretion of PMN chemoattracting factor(s) (Fig. 5F) were significantly inhibited by BAY11-7082 or etanercept. In addition, the levels of expression of Gb_3 induced by Stx1 in LPS-sensitized ASTs (Fig. 5D) as well as the internalization of Stx1 in LPS-sensitized ASTs (Fig. 5E) were reduced by blocking TNF-α or inhibiting NF-κB activation. Together, these results show that AST-derived TNF-α and NF-κB activation contribute to the enhanced response induced by Stx1 in LPS-sensitized ASTs.

DISCUSSION

CNS complications are recognized as a major determinant of morbidity and mortality in the acute phase of STEC infections. Although the pathogenesis of CNS involvement is not yet fully understood, the disruption and/or increased permeability of the BBB and neuronal disturbance, as a consequence of BEC injury, are central events in the CNS complications observed during the acute phase of HUS (48).

ASTs comprise 55 to 60% of total human brain cells (13) and are involved in virtually every type of brain pathology. This is due in part to their inflammatory potential, since ASTs are considered to be the primary cellular source of TNF-α and NO, two mediators associated with CNS pathologies (16, 29).

Therefore, the cellular response of ASTs to Stx1 and LPS is essential to understand the neuropathology observed for severe cases of HUS. Although Stx-induced toxicity on neurons and BECs was demonstrated previously (20, 23), little is known about the effects of Stx on ASTs. In this regard, it was recently documented that the intracerebroventricular administration of Stx2 to adult rats causes AST activation, although its effects on the AST inflammatory response were not determined (7, 23).

We found that maximal effects induced by Stx1 treatment were observed when ASTs were prestimulated with LPS. Toxin binding to Gb_3 is the primary determinant of the cytotoxic and pathological effects of Stx proteins (33). Previous works highlighted the role of proinflammatory agents in enhancing sensitivity to Stx-induced effects by the upregulation of Gb_3 expression in different target cells including BECs (11, 45). Our data extend these observations to ASTs, since LPS preincubation enhanced Gb_3 expression and, consequently, Stx1 internalization. Interestingly, maximal Gb_3 expression was observed with Stx1 stimulation of LPS-primed ASTs, suggesting that the modulation of Gb_3 may be mediated by a positive-feedback mechanism. To our knowledge, this is the first evidence for a role of Stx1 in the modulation of its own receptor.

An early inflammatory response, assessed as TNF-α and NO release and PMN-chemoattractant activity, was induced by Stx1 on LPS-sensitized ASTs, while AST activation (increased GFAP expression levels) and cell death were late consequences of the Stx1 treatment of LPS-sensitized ASTs. Since TNF-α secretion is induced upon LPS stimulation through the activation of NF-κB, we examined the role of NF-κB and endogenously secreted TNF-α in the LPS sensitization of ASTs to Stx1-mediated effects. We found that both AST activation and cell death were abrogated by the suppression of NF-κB activation or the blockade of endogenous TNF-α activity. In agreement with these results, TNF-α as well as NF-κB activation have been implicated in the regulation of GFAP expression (25). Additionally, the exposure of ASTs to different death stimuli induces NF-κB activation, and NF-κB inhibitors blocked AST cell death (40).

Moreover, we showed that the increased level of expression

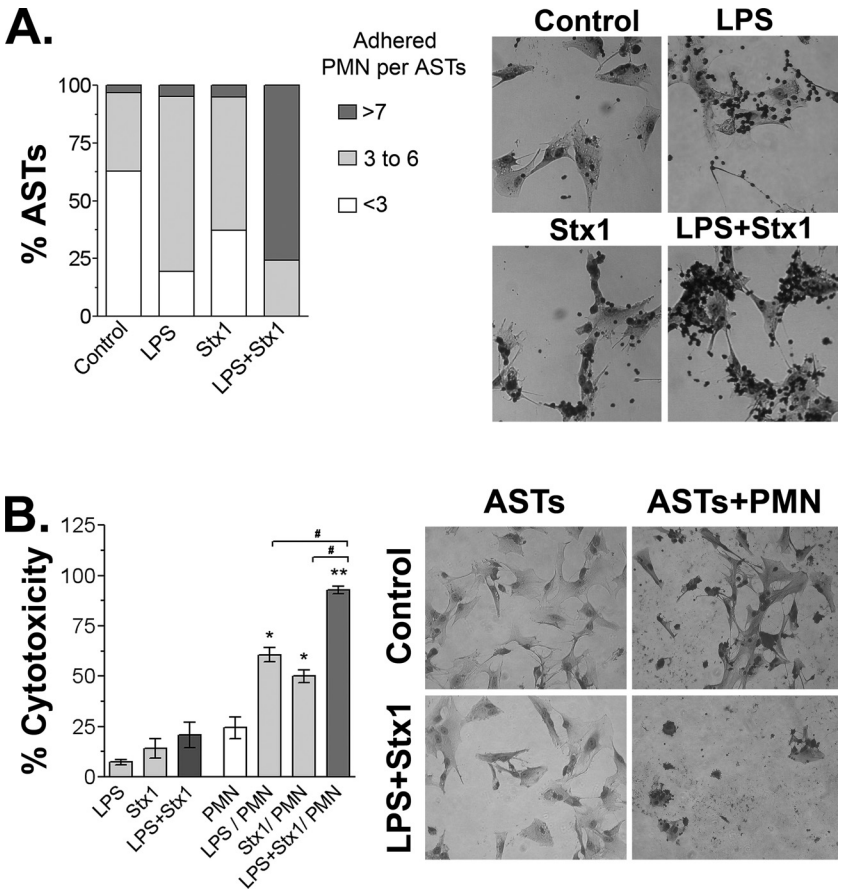

FIG. 4. Stx1 increases adhesiveness and sensitivity to PMN-mediated toxicity in LPS-sensitized ASTs. ASTs were cultured in complete medium alone (control) or in the presence of 0.5 μg/ml LPS (0 to 42 h) and/or 10 ng/ml Stx1 (18 h after LPS pretreatment). ASTs were coincubated with syngeneic PMN (24 h after Stx1 was added). ASTs with adherent PMN were analyzed at 3 h (A) and PMN-mediated cytotoxicity was determined at 8 h (B) by light microscopy (magnification, ×600). (A) Percentage of ASTs bearing PMN. The number of ASTs bearing PMN was scored in three randomly selected microscope fields (~50 ASTs; $n = 3$), and data are grouped as the number of ASTs with <3, 3 to 6, or >7 adhered PMN. Stratified distribution analyses of these data were used for statistical analysis (χ^2 test) ($P < 0.01$ for the control versus LPS or Stx1; $P < 0.001$ for control versus LPS and Stx1; $P < 0.01$ for LPS and Stx1 versus LPS or Stx1). Representative gray-scale micrographs of one representative independent experiment are depicted (right). (B) The percent specific cytotoxicity was determined by microscopic quantification. The bar graph (mean ± SEM) summarizes data from four independent experiments. *, $P < 0.05$ for LPS or Stx1/PMN versus PMN; **, $P < 0.001$ for LPS and Stx1/PMN versus PMN; #, $P < 0.005$ for LPS and Stx1/PMN versus LPS or Stx1/PMN. Micrographs of one representative independent experiment are depicted (right).

of the Gb_3 receptor observed after LPS and Stx1 stimulation was also dependent on the NF-κB/TNF-α pathway, although the mechanism involved has not been established. However, it was demonstrated using human BECs and intestinal epithelial cells that TNF-α increases Gb_3 expression levels by the generation of lactosylceramide (LacCer) through the activation of lactosylceramide synthase (39). This pathway could also mediate Gb_3 upregulation on ASTs, as it was shown previously that TNF-α stimulation increases the intracellular levels of LacCer in these cells (32). In summary, our results reveal that TNF-α acts autocrinally/paracrinally as a pivotal effector molecule for amplifying Stx1 effects on LPS-sensitized ASTs. These effects are likely to occur by enhancing Gb_3 expression and Stx1 internalization.

Although Stx proteins have been classically considered to be ribosome-intoxicating proteins, exerting their effects on cells by blocking new-protein synthesis, recent data indicate that subtoxic amounts of Stx have only minor effects on overall protein synthesis but have dramatic effects on gene regulation, causing increased levels of expression of hallmark proadhesive, prothrombotic, and inflammatory genes, for example, in endothelial cells (34). This seems to be the case for ASTs under nonsensitized conditions, where Stx by itself was able to cause a slight but statistically significant increase in TNF-α secretion and PMN migration and adhesion but failed to induce cell death or GFAP upregulation.

Activated PMN play a prominent role in neuropathology. They can rapidly infiltrate the injured brain parenchyma and release proteases and potentially toxic substances (3). For HUS patients, a high peripheral PMN count at presentation was associated largely with a poor prognosis (17). Previous reports established that several chemokines and chemokine receptors are expressed in astroglial cells, either constitutively or induced by inflammatory mediators. (28).

Our data demonstrate that ASTs treated with LPS or Stx1 stimulate PMN migration and adhesion in ASTs, resulting in

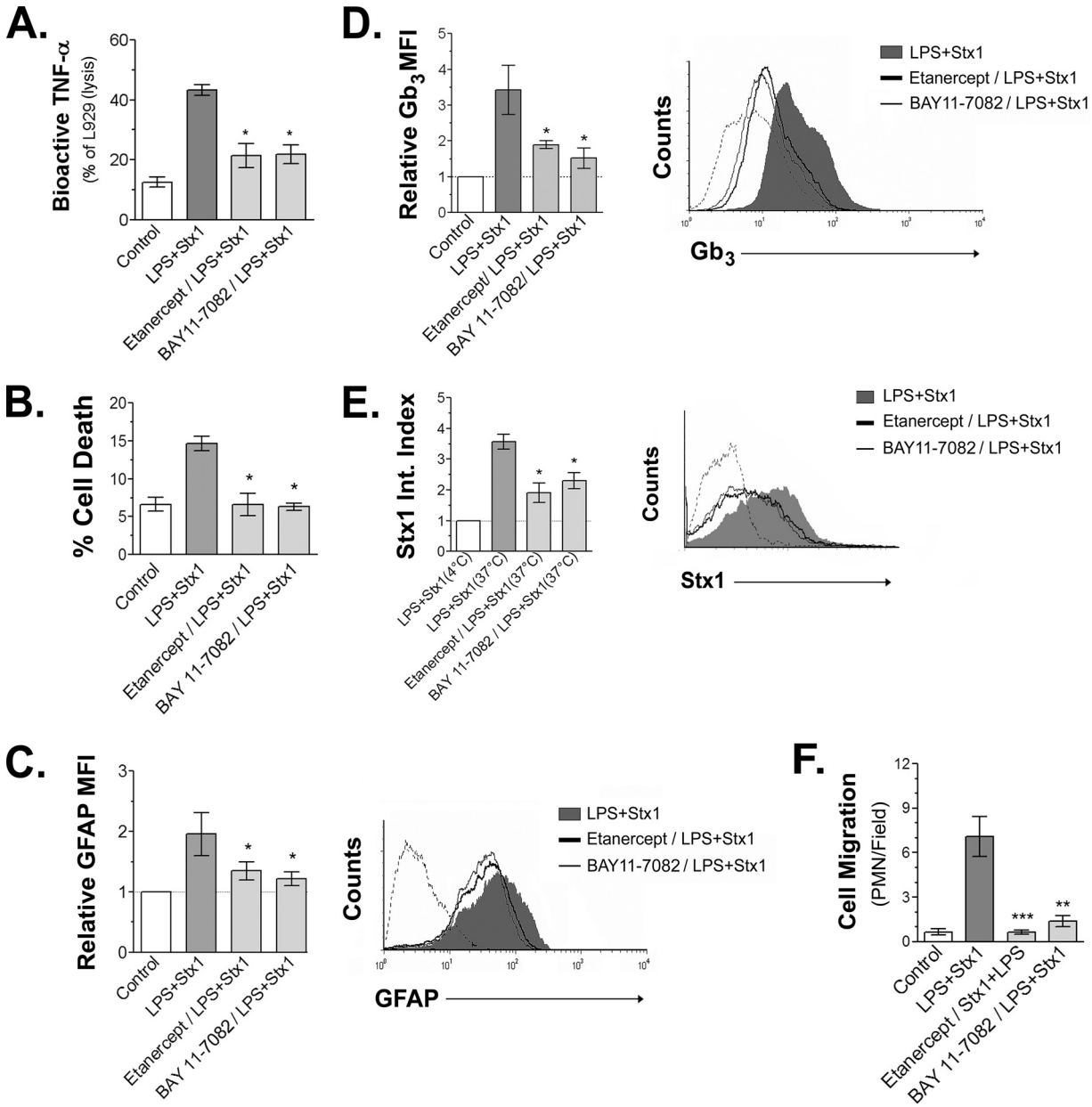

FIG. 5. Effects of Stx1 on LPS-sensitized ASTs are abrogated by NF-κB or TNF-α inhibition. ASTs were treated with TNF-α binding blocker etanercept or the NF-κB inhibitor BAY11-7082 before treatment with LPS and Stx1. ASTs (B, C, D, and E) or AST conditioned medium (A and F) was assayed as described in the legend of Fig. 1, 2, and 3A and C. (A) TNF-α bioactivity (mean ± SEM). *, $P < 0.05$ for LPS and Stx1 versus etanercept or BAY11-7082/LPS and Stx1 ($n = 4$). (B) Percent AST death (mean ± SEM). *, $P < 0.05$ for LPS and Stx1 versus etanercept or BAY11-7082/LPS and Stx1 ($n = 4$). (C) Relative MFI of intracellular GFAP immunostaining (mean ± SEM). *, $P < 0.05$ for LPS and Stx1 versus etanercept or BAY11-7082/LPS and Stx1 ($n = 4$). A representative histogram plot analysis is depicted (right). (D) Relative MFI of the Stx1 receptor Gb_3 (mean ± SEM; $n = 4$). A representative histogram plot analysis is depicted (right). (E) Stx1 internalization index (mean ± SEM). *, $P < 0.05$ for LPS versus etanercept or BAY11-7082/LPS ($n = 4$). A representative histogram is depicted (right). (F) Cell migration evaluation (mean ± SEM; $n = 5$). ***, $P < 0.005$ for LPS and Stx1 versus etanercept/LPS and Stx1; **, $P < 0.01$ for LPS and Stx1 versus BAY11-7082/LPS and Stx1.

AST toxicity. Again, maximal effects were reached with Stx1 on LPS-sensitized ASTs. This indicates that AST-released factors following treatment with LPS/Stx1 may activate PMN directly or indirectly, thus leading to AST toxicity. In this sense, activated PMN could contribute to the brain inflammatory response and participate in the secondary damage after BBB disruption in HUS. In line with this hypothesis, the prevention of PMN vascular adhesion/invasion is neuroprotective in some CNS pathologies (10, 47). The effect of traces of LPS or Stx1 in AST-conditioned medium on PMN activation cannot be completely ruled out. However, it was demonstrated previously that even after PMN priming with LPS, TNF-α, or IL-8, Stx fails to activate PMN (18, 22). Moreover, the enhanced PMN-mediated toxicity observed after the combined treatment (LPS

and Stx1) compared to that of LPS alone supports the finding that the observed effects may be due to an AST-derived factor(s) (Fig. 4B).

The *in vivo* relevance of our findings is supported by data from studies where the local production of TNF-α in mouse brains after STEC infection was previously described, although the cellular source has not been determined (30). Moreover, it was reported previously that microinjection of TNF-α in the brain induces PMN accumulation and adherence to blood vessels (26). Our results prompted us to propose that ASTs are an important source of inflammatory mediators accounting for increased BEC susceptibility to Stx-induced effects and therefore contributing to the BBB disruption and neurotoxicity in HUS.

The results presented herein suggest that NF-κB and TNF-α could be target molecules to prevent or diminish the CNS complications observed for HUS patients. Several *in vivo* studies of different CNS pathologies demonstrated that the suppression of AST activation and their inflammatory response resulted in reduced disease severity and improved functional recovery (8, 38). In addition, recent reports showed clinical improvement for patients with Alzheimer's disease and related disorders following the perispinal administration of etanercept, suggesting that etanercept has the ability to penetrate into the cerebrospinal fluid in the brain at a therapeutically effective concentration (41–43).

Further *in vivo* studies should clarify whether the inhibition of NF-κB signaling or TNF-α production in ASTs results in protective effects and if the NF-κB pathway is a convenient new target for the development of therapeutic strategies for the treatment of CNS complications in HUS patients.

ACKNOWLEDGMENTS

This work was supported by grants from the Agencia Nacional de Promoción Científica y Tecnológica, the Consejo Nacional de Investigaciones Científicas y Técnicas, and Alberto J. Roemmers.

We thank Laura Pasquini, Yanina Pasquini, Nora Galassi, and Marta Felippo for their excellent technical assistance. We also thank Susana Fink for manuscript revision.

We declare no conflict of interest.

REFERENCES

1. **Abbott, N. J.** 2000. Inflammatory mediators and modulation of blood-brain barrier permeability. Cell. Mol. Neurobiol. **20:**131–147.
2. **Arthur, F. E., R. R. Shivers, and P. D. Bowman.** 1987. Astrocyte-mediated induction of tight junctions in brain capillary endothelium: an efficient in vitro model. Brain Res. **433:**155–159.
3. **Barone, F. C., L. M. Hillegass, W. J. Price, R. F. White, E. V. Lee, G. Z. Feuerstein, H. M. Sarau, R. K. Clark, and D. E. Griswold.** 1991. Polymorphonuclear leukocyte infiltration into cerebral focal ischemic tissue: myeloperoxidase activity assay and histologic verification. J. Neurosci. Res. **29:**336–345.
4. **Beck, D. W., H. V. Vinters, M. N. Hart, and P. A. Cancilla.** 1984. Glial cells influence polarity of the blood-brain barrier. J. Neuropathol. Exp. Neurol. **43:**219–224.
5. **Betsuyaku, T., F. Liu, R. M. Senior, J. S. Haug, E. J. Brown, S. L. Jones, K. Matsushima, and D. C. Link.** 1999. A functional granulocyte colony-stimulating factor receptor is required for normal chemoattractant-induced neutrophil activation. J. Clin. Invest. **103:**825–832.
6. **Blanc, E. M., A. J. Bruce-Keller, and M. P. Mattson.** 1998. Astrocytic gap junctional communication decreases neuronal vulnerability to oxidative stress-induced disruption of Ca2+ homeostasis and cell death. J. Neurochem. **70:**958–970.
7. **Boccoli, J., C. F. Loidl, J. J. Lopez-Costa, V. P. Creydt, C. Ibarra, and J. Goldstein.** 2008. Intracerebroventricular administration of Shiga toxin type 2 altered the expression levels of neuronal nitric oxide synthase and glial fibrillary acidic protein in rat brains. Brain Res. **1230:**320–333.
8. **Brambilla, R., T. Persaud, X. Hu, S. Karmally, V. I. Shestopalov, G. Dvoriantchikova, D. Ivanov, L. Nathanson, S. R. Barnum, and J. R. Bethea.** 2009. Transgenic inhibition of astroglial NF-kappa B improves functional outcome in experimental autoimmune encephalomyelitis by suppressing chronic central nervous system inflammation. J. Immunol. **182:**2628–2640.
9. **Chen, Y., R. M. McCarron, N. Azzam, J. Bembry, C. Reutzler, F. A. Lenz, and M. Spatz.** 2000. Endothelin-1 and nitric oxide affect human cerebromicrovascular endothelial responses and signal transduction. Acta Neurochir. Suppl. **76:**131–135.
10. **Connolly, E. S., Jr., C. J. Winfree, T. A. Springer, Y. Naka, H. Liao, S. D. Yan, D. M. Stern, R. A. Solomon, J. C. Gutierrez-Ramos, and D. J. Pinsky.** 1996. Cerebral protection in homozygous null ICAM-1 mice after middle cerebral artery occlusion. Role of neutrophil adhesion in the pathogenesis of stroke. J. Clin. Invest. **97:**209–216.
11. **Eisenhauer, P. B., P. Chaturvedi, R. E. Fine, A. J. Ritchie, J. S. Pober, T. G. Cleary, and D. S. Newburg.** 2001. Tumor necrosis factor alpha increases human cerebral endothelial cell Gb3 and sensitivity to Shiga toxin. Infect. Immun. **69:**1889–1894.
12. **Endo, Y., K. Tsurugi, T. Yutsudo, Y. Takeda, T. Ogasawara, and K. Igarashi.** 1988. Site of action of a Vero toxin (VT2) from Escherichia coli O157:H7 and of Shiga toxin on eukaryotic ribosomes. RNA N-glycosidase activity of the toxins. Eur. J. Biochem. **171:**45–50.
13. **Eng, L. F., and R. S. Ghirnikar.** 1994. GFAP and astrogliosis. Brain Pathol. **4:**229–237.
14. **Eriksson, K. J., S. G. Boyd, and R. C. Tasker.** 2001. Acute neurology and neurophysiology of haemolytic-uraemic syndrome. Arch. Dis. Child. **84:**434–435.
15. **Exeni, R. A., G. C. Fernandez, and M. S. Palermo.** 2007. Role of polymorphonuclear leukocytes in the pathophysiology of typical hemolytic uremic syndrome. ScientificWorldJournal **7:**1155–1164.
16. **Fan, L., P. R. Young, F. C. Barone, G. Z. Feuerstein, D. H. Smith, and T. K. McIntosh.** 1996. Experimental brain injury induces differential expression of tumor necrosis factor-alpha mRNA in the CNS. Brain Res. Mol. Brain Res. **36:**287–291.
17. **Fernandez, G. C., S. A. Gomez, M. V. Ramos, L. Bentancor, R. J. Fernandez-Brando, V. I. Landoni, L. Lopez, F. Ramirez, M. Diaz, M. Alduncin, I. Grimoldi, R. Exeni, M. A. Isturiz, and M. S. Palermo.** 2007. The functional state of neutrophils correlates with the severity of renal dysfunction in children with hemolytic uremic syndrome. Pediatr. Res. **61:**123–128.
18. **Fernandez, G. C., S. A. Gomez, C. J. Rubel, L. V. Bentancor, P. Barrionuevo, M. Alduncin, I. Grimoldi, R. Exeni, M. A. Isturiz, and M. S. Palermo.** 2005. Impaired neutrophils in children with the typical form of hemolytic uremic syndrome. Pediatr. Nephrol. **20:**1306–1314.
19. **Fujii, J., Y. Kinoshita, Y. Yamada, T. Yutsudo, T. Kita, T. Takeda, and S. Yoshida.** 1998. Neurotoxicity of intrathecal Shiga toxin 2 and protection by intrathecal injection of anti-Shiga toxin 2 antiserum in rabbits. Microb. Pathog. **25:**139–146.
20. **Fujii, J., T. Kita, S. Yoshida, T. Takeda, H. Kobayashi, N. Tanaka, K. Ohsato, and Y. Mizuguchi.** 1994. Direct evidence of neuron impairment by oral infection with verotoxin-producing Escherichia coli O157:H− in mitomycin-treated mice. Infect. Immun. **62:**3447–3453.
21. **Fukuda, M., K. Kitaichi, F. Abe, Y. Fujimoto, K. Takagi, T. Morishima, and T. Hasegawa.** 2005. Altered brain penetration of diclofenac and mefenamic acid, but not acetaminophen, in Shiga-like toxin II-treated mice. J. Pharmacol. Sci. **97:**525–532.
22. **Geelen, J. M., T. J. van der Velden, D. M. Te Loo, O. C. Boerman, L. P. van den Heuvel, and L. A. Monnens.** 2007. Lack of specific binding of Shiga-like toxin (verocytotoxin) and non-specific interaction of Shiga-like toxin 2 antibody with human polymorphonuclear leucocytes. Nephrol. Dial. Transplant. **22:**749–755.
23. **Goldstein, J., C. F. Loidl, V. P. Creydt, J. Boccoli, and C. Ibarra.** 2007. Intracerebroventricular administration of Shiga toxin type 2 induces striatal neuronal death and glial alterations: an ultrastructural study. Brain Res. **1161:**106–115.
24. **Kacem, K., P. Lacombe, J. Seylaz, and G. Bonvento.** 1998. Structural organization of the perivascular astrocyte endfeet and their relationship with the endothelial glucose transporter: a confocal microscopy study. Glia **23:**1–10.
25. **Lin, S. T., Y. Wang, Y. Xue, D. C. Feng, Y. Xu, and L. Y. Xu.** 2008. Tetrandrine suppresses LPS-induced astrocyte activation via modulating IKKs-IkappaBalpha-NF-kappaB signaling pathway. Mol. Cell. Biochem. **315:**41–49.
26. **Lotan, M., A. Solomon, S. Ben-Bassat, and M. Schwartz.** 1994. Cytokines modulate the inflammatory response and change permissiveness to neuronal adhesion in injured mammalian central nervous system. Exp. Neurol. **126:**284–290.
27. **McCarthy, K. D., and J. de Vellis.** 1980. Preparation of separate astroglial and oligodendroglial cell cultures from rat cerebral tissue. J. Cell Biol. **85:**890–902.
28. **Meeuwsen, S., C. Persoon-Deen, M. Bsibsi, R. Ravid, and J. M. van Noort.** 2003. Cytokine, chemokine and growth factor gene profiling of cultured human astrocytes after exposure to proinflammatory stimuli. Glia **43:**243–253.

29. **Murphy, S.** 2000. Production of nitric oxide by glial cells: regulation and potential roles in the CNS. Glia **29:**1–13.
30. **Okayama, A., K. Mikasa, N. Matsui, N. Higashi, M. Miyamoto, and E. Kita.** 2004. An interventional approach to block brain damage caused by Shiga toxin-producing Escherichia coli infection, by use of a combination of phosphodiesterase inhibitors. J. Infect. Dis. **190:**2129–2136.
31. **O'Neill, L. A., and C. Kaltschmidt.** 1997. NF-kappa B: a crucial transcription factor for glial and neuronal cell function. Trends Neurosci. **20:**252–258.
32. **Pannu, R., A. K. Singh, and I. Singh.** 2005. A novel role of lactosylceramide in the regulation of tumor necrosis factor alpha-mediated proliferation of rat primary astrocytes. Implications for astrogliosis following neurotrauma. J. Biol. Chem. **280:**13742–13751.
33. **Paton, J. C., and A. W. Paton.** 1998. Pathogenesis and diagnosis of Shiga toxin-producing Escherichia coli infections. Clin. Microbiol. Rev. **11:**450–479.
34. **Petruzziello, T. N., I. A. Mawji, M. Khan, and P. A. Marsden.** 2009. Verotoxin biology: molecular events in vascular endothelial injury. Kidney Int. Suppl. **2009:**S17–S19.
35. **Proulx, F., E. G. Seidman, and D. Karpman.** 2001. Pathogenesis of Shiga toxin-associated hemolytic uremic syndrome. Pediatr. Res. **50:**163–171.
36. **Ramegowda, B., J. E. Samuel, and V. L. Tesh.** 1999. Interaction of Shiga toxins with human brain microvascular endothelial cells: cytokines as sensitizing agents. J. Infect. Dis. **180:**1205–1213.
37. **Shiau, M. Y., H. L. Chiou, Y. L. Lee, T. M. Kuo, and Y. H. Chang.** 2001. Establishment of a consistent L929 bioassay system for TNF-alpha quantitation to evaluate the effect of lipopolysaccharide, phytomitogens and cytodifferentiation agents on cytotoxicity of TNF-alpha secreted by adherent human mononuclear cells. Mediators Inflamm. **10:**199–208.
38. **Sommer, C., M. Schafers, M. Marziniak, and K. V. Toyka.** 2001. Etanercept reduces hyperalgesia in experimental painful neuropathy. J. Peripher. Nerv. Syst. **6:**67–72.
39. **Stricklett, P. K., A. K. Hughes, Z. Ergonul, and D. E. Kohan.** 2002. Molecular basis for up-regulation by inflammatory cytokines of Shiga toxin 1 cytotoxicity and globotriaosylceramide expression. J. Infect. Dis. **186:**976–982.
40. **Takuma, K., E. Lee, M. Kidawara, K. Mori, Y. Kimura, A. Baba, and T. Matsuda.** 1999. Apoptosis in Ca2+ reperfusion injury of cultured astrocytes: roles of reactive oxygen species and NF-kappaB activation. Eur. J. Neurosci. **11:**4204–4212.
41. **Tobinick, E.** 2008. Perispinal etanercept produces rapid improvement in primary progressive aphasia: identification of a novel, rapidly reversible TNF-mediated pathophysiologic mechanism. Medscape J. Med. **10:**135.
42. **Tobinick, E. L., and H. Gross.** 2008. Rapid cognitive improvement in Alzheimer's disease following perispinal etanercept administration. J. Neuroinflammation **5:**2.
43. **Tobinick, E. L., and H. Gross.** 2008. Rapid improvement in verbal fluency and aphasia following perispinal etanercept in Alzheimer's disease. BMC Neurol. **8:**27.
44. **Utsunomiya, I., J. Ren, K. Taguchi, T. Ariga, T. Tai, Y. Ihara, and T. Miyatake.** 2001. Immunohistochemical detection of verotoxin receptors in nervous system. Brain Res. Brain Res. Protoc. **8:**99–103.
45. **van Setten, P. A., V. W. van Hinsbergh, T. J. van der Velden, N. C. van de Kar, M. Vermeer, J. D. Mahan, K. J. Assmann, L. P. van den Heuvel, and L. A. Monnens.** 1997. Effects of TNF alpha on verocytotoxin cytotoxicity in purified human glomerular microvascular endothelial cells. Kidney Int. **51:**1245–1256.
46. **Wang, J. Y., A. Y. Shum, C. C. Chao, and J. S. Kuo.** 2000. Production of macrophage inflammatory protein-2 following hypoxia/reoxygenation in glial cells. Glia **32:**155–164.
47. **Yamasaki, Y., Y. Matsuo, J. Zagorski, N. Matsuura, H. Onodera, Y. Itoyama, and K. Kogure.** 1997. New therapeutic possibility of blocking cytokine-induced neutrophil chemoattractant on transient ischemic brain damage in rats. Brain Res. **759:**103–111.
48. **Zoja, C., D. Corna, C. Farina, G. Sacchi, C. Lingwood, M. P. Doyle, V. V. Padhye, M. Abbate, and G. Remuzzi.** 1992. Verotoxin glycolipid receptors determine the localization of microangiopathic process in rabbits given verotoxin-1. J. Lab. Clin. Med. **120:**229–238.

Editor: B. A. McCormick